ROTOR FAULTS DETECTION IN SQUIRREL-CAGE INDUCTION MOTORS BY CURRENT SIGNATURE ANALYSIS

SZABÓ Loránd – DOBAI Jenő Barna – BIRÓ Károly Ágoston

Technical University of Cluj (Romania)
400750 Cluj, P.O. Box 358, Romania
e-mail: Lorand.Szabo@mae.utcluj.ro

Abstract: The condition monitoring of the electrical machines can significantly reduce the costs of maintenance by allowing the early detection of faults, which could be expensive to repair. In this paper some results on non-invasive detection of broken rotor bars in squirrel-cage induction motors are presented. The applied method is the so-called motor current signature analysis (MCSA) which utilises the results of spectral analysis of the stator current. The diagnosis procedure was performed by using virtual instruments (VIs). The significant presence of some well-defined sideband frequencies in the harmonic spectrum of the measured line current clearly indicates the rotor faults of the induction machine. The theoretical basis of this method was proved by laboratory tests.

Keywords: condition monitoring, fault detection, motor current signature analysis (MCSA), squirrel-cage induction motor, virtual instrument (VI).

1. INTRODUCTION

Induction motors (see Fig. 1) play an important role in the safe and efficient operation of industrial plants. Usually they are designed for 30 years fault-free lifetime, but most of them are not available at all times.

Figure 1 – Induction motor

Many electric machine components are especially susceptible to failures. The stator windings are subject to insulation break-down caused by mechanical vibration, heat, age, damage during installation, etc. The machine rotor bars and end rings can be broken by the various stresses that act on the rotor. Machine bearings are subject to excessive wear and damage caused by inadequate lubrication, asymmetric loading, or misalignment.

In many applications these failures of the electrical machines can shut down an entire industrial process. Such unplanned machine shut downs cost both time and money that could be avoided if an early warning system is available against impending

failures. Such a system could also improve process safety, a key factor in many industrial environments. Fault detection and diagnosis schemes are intended to provide advanced warnings of incipient faults, so that corrective action can be taken without detrimental interruption to processes. Fault diagnosis of electrical machines can lead to greater plant availability, extended plant life, higher quality products, and smoother plant operations [1].

Numerous fault detection methods have been proposed to identify the above faults. The fault detection methods involve several different types of fields of science and technology. They are generally performed by mechanical and/or electrical monitoring.

The most frequent used detection methods are [2]:

- Motor current signature analysis (MCSA),
- Acoustic noise measurements,
- Model, artificial intelligence and neural network based techniques,
- Noise and vibration monitoring,
- Electromagnetic field monitoring using search coils, or coils wound around motor shafts (axial flux related detection),
- Temperature measurements,
- Infrared recognition,
- Radio frequency (RF) emissions monitoring,
- Chemical analysis, etc.

For the detection of the induction motor's rotor faults here the motor current signature analysis method was applied.

2. MOTOR CURRENT SIGNATURE ANALYSIS (MCSA)

One of the most frequently used fault detection methods is the motor current signature analysis (MCSA). This technique depends upon locating by spectrum analysis specific harmonic components in the line current produced of unique rotating flux components caused by faults such as broken rotor bars, air-gap eccentricity and shorted turns in stator windings, etc. Note that only one current transducer is required for this method, and it can be in any one of the three phases. The motor current signature analysis method can detect these problems at an early stage and thus avoid secondary damage and complete failure of the motor. Another advantage of this method is that it can be also applied online.

An idealised current spectrum is shown in Fig. 2. The two slip frequency sidebands due to broken rotor bars near the main harmonic can be clearly observed.

Usually a decibel (dB) versus frequency spectrum is used in order to give a wide dynamic range and to detect the unique current signature patterns that are characteristic of different faults [3, 4].

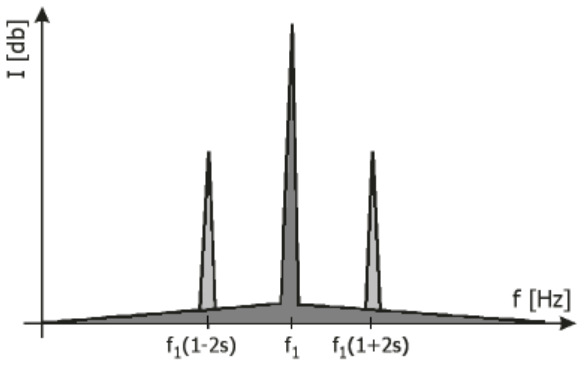

Figure 2 – Idealised current spectrum

The fundamental reason for the appearance of the above-mentioned sideband frequencies in the power spectrum will be discussed next.

In the three-phase induction motor under perfectly balanced conditions (healthy motor) only a forward rotating magnetic field is produced, which rotates at synchronous speed, $n_1 = f_1/p$, where f_1 is the supply frequency and p the pole-pairs of the stator windings. The rotor of the induction motor always rotates at a speed (n) less than the synchronous speed. The slip, $s = (n_1 - n)/n_1$, is the measure of the slipping back of the rotor regarding to the rotating field. The slip speed ($n_2 = n_1 - n = sn_1$) is the actual difference in between the speed of the rotating magnetic field and the actual speed of the rotor.

The frequency of the rotor currents is called the slip frequency and is given by:

$$f_2 = n_2\, p = s\, n_1\, p \tag{1}$$

The speed of the rotating magnetic field produced by the current carrying rotor conductors with respect to the stationary stator winding is given by:

$$n + n_2 = n + n_1 - n = n_1 \tag{2}$$

With respect to a stationary observer on the fixed stator winding, then the speed of the rotating magnetic field from the rotor equals the speed of the stator rotating magnetic field, namely, the synchronous speed.

Both mentioned fields are locked together to give a steady torque production by the induction motor.

With broken rotor bars in the motor there is an additional, backward rotating magnetic field produced, which is rotating at the slip speed with respect to the rotor.

The backward rotating magnetic field speed produced by the rotor due to broken bars and with respect to the rotor is:

$$n_b = n - n_2 = n_1(1-s) - sn_1 = n_1 - 2sn_1 = n_1(1-2s) \tag{3}$$

The stationary stator winding now sees a rotating field at:

$$n_b = n_1(1-2s) \tag{4}$$

or expressed in terms of frequency:

$$f_b = f_1(1-2s) \tag{5}$$

This means that a rotating magnetic field at that frequency cuts the stator windings and induces a current at that frequency (f_b). This in fact means that f_b is a twice slip frequency component spaced $2sf_1$ down from f_1. Thus speed and torque oscillations occur at $2sf_1$, and this induces an upper sideband at $2sf_1$ above f_1.

Classical twice slip frequency sidebands therefore occur at $\pm 2sf_1$ around the supply frequency [3]:

$$f_b = (1 \pm 2s) f_1 \tag{6}$$

While the lower sideband is specifically due to broken bar, the upper sideband is due to consequent speed oscillation. In fact, several papers shows that broken bars actually give rise to a sequence of such sidebands given by [2]:

$$f_b = (1 \pm 2ks) f_1, \quad k = 1, 2, 3\ldots \tag{7}$$

Therefore the appearance in the harmonic spectrum of the sidebands frequencies given by (6) or (7) clearly indicates a rotor fault of the induction machine.

3. ROTOR FAULTS DETECTION

Broken rotor bars can be a serious problem with certain induction motors due to arduous duty cycles. Although broken rotor bars do not initially cause an induction motor to fail, there can be serious secondary effects. The fault mechanism can result in broken parts of the bar hitting the end winding or stator core of a high voltage motor at a high velocity. This can cause serious mechanical damage to the insulation and a consequential winding failure may follow, resulting in a costly repair and lost production [3].

Broken rotor bars or end rings can be caused by the following:

- Direct-on-line starting duty cycles for which the rotor cage winding was not designed to withstand causes high thermal and mechanical stresses.
- Pulsating mechanical loads such as reciprocating compressors or coal crushers (etc.) can subject the rotor cage to high mechanical stresses.
- Imperfections in the manufacturing process of the rotor cage.

In order to make several measurements with healthy and faulty squirrel-cage induction motors a modern laboratory test bench was set up [5]. It consists of two coupled electrical machines: the machine to be tested and a DC machine fed by a controlled rectifier used for loading.

Several sensors were coupled to the motor. Hall effect transducers measured the voltages and the currents. An angular incremental position could measure the position and the speed of the motor. All the sensor signals were collected by the data board.

Several virtual instruments (VIs) were built up in LabVIEW [6]. These VIs were used both for controlling the test measurements and data acquisition, and for the data processing [7]. The VI created for processing and analysing the acquired data from the test bench is given in Fig. 3.

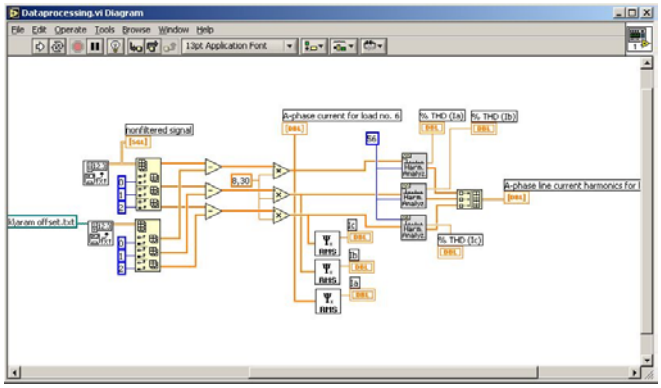

Figure 3 – The data processing VI's diagram

The rated data of the tested three-phase squirrel cage induction machine were: 1.5 kW, 220/380 V (Δ/Y), 6.18/3.56 A (Δ/Y) and 1410 r/min.

Tests were carried out for seven different loads with the healthy motor, and with similar motors having up to 5 broken rotor bars. The rotor faults were provoked interrupting the rotor bars by drilling into the rotor (see Fig. 4).

The measured current signals were processed using the Fast Fourier Transformation (FFT). The power density of the measured phase currents was plotted. The results obtained for the healthy motor and those having rotor faults were compared, especially looking for the sideband components having the frequencies given by equation (6) and (7).

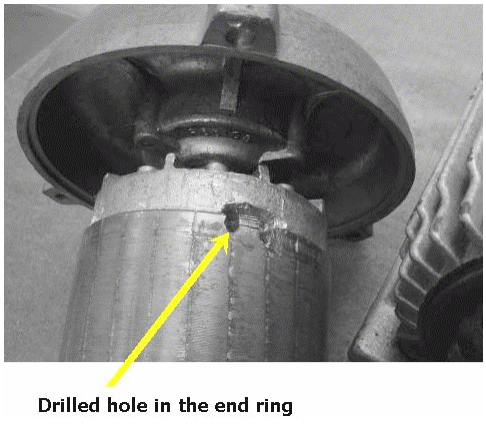

Figure 4 – The faulty rotor

4. RESULTS AND CONCLUSIONS

From the huge number of obtained results here only the most significant ones will be presented. The power densities of the measured line current at no-load for 3 conditions of the studied motor are given in Fig. 5.

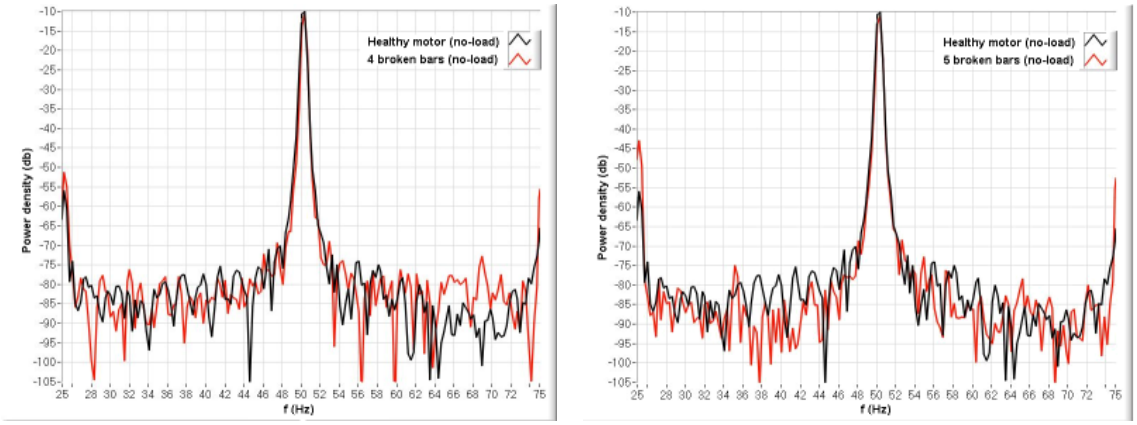

a) healthy and 4 broken bars motor **b) healthy and 5 broken bars motor**

Figure 5 – The power density of the measured line current at no-load

A it can be seen from the figure, the detection of the searched slip frequency sidebands at no-load (and also at little loads) is too difficult, since the current in the rotor bars is small. The most eloquent results were obtained at great loads, especially near the rated load.

In Fig. 6 the power density of the measured line current is given for the motor having 4, respectively 5 broken bars at the two above mentioned loads. The sideband frequency components of the power spectrum are marked with circles.

For example, for the motor having 5 broken bars at load no. 4 (65% of the rated load) the measured speed of the motor was 1455 r/min. At this speed the slip is 0,03. The corresponding sideband frequencies computed with equation (7) for k=1 and k=2 are: 44, 47, 53 and 56 Hz. At the rated load (no. 6) the speed is less, 1425 r/min, which means that the slip is greater, equal to 0,05. In this case the computed sideband frequencies are: 40, 45, 55 and 60 Hz.

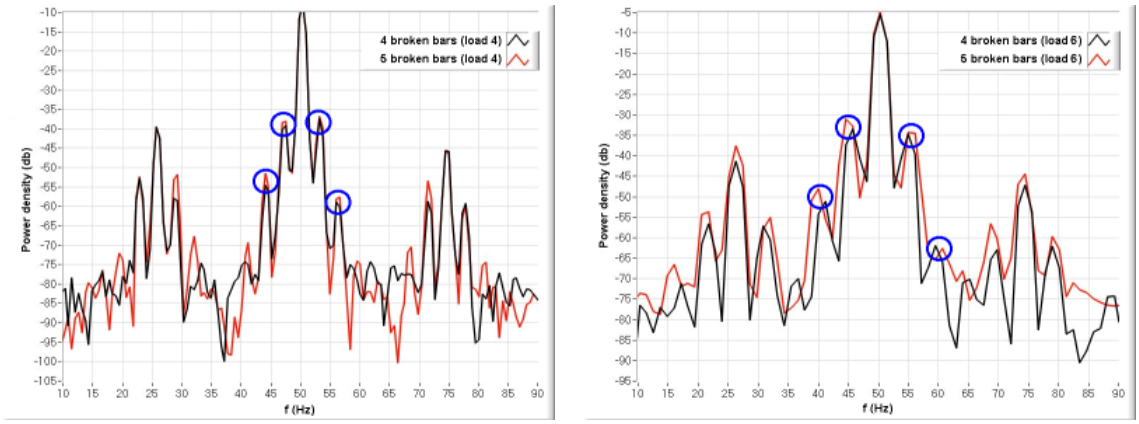

a) Motor at load no. 4 **b) Motor at load no. 6**

Figure 6 – The power density of the measured line current of the motors having 4, respectively 5 broken bars, and the observed sideband frequency components

As it can be seen, all the expected sideband frequency harmonics can be observed in the figures. Thus the above presented theory of the slip frequency sidebands is proved by measurements.

These sideband frequencies are function of the slip, so they are changing with the speed (implicitly with the load). This phenomenon can be clearly observed from Fig. 7, where the power density of the measured currents for the motor having 4 broken bars are plotted for three different cases. As it can be seen, as the load is increased, the magnitude of the sideband frequency components is also increasing.

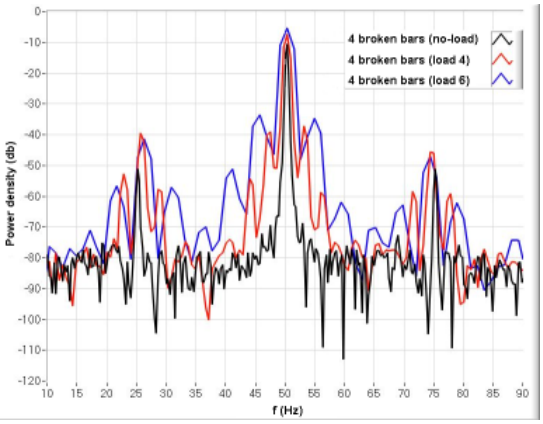

Figure 7 – Comparative power densities of the measured line current

As in this paper was stated out the presence of the slip frequency sidebands indicates the existence of the broken rotor bars. They magnitude is function of the number of the broken bars. To found a relation between these magnitudes and the number of the broken bars will be the next task for our research team.

5. ACKNOWLEDGEMENTS

The work was possible due to the support given by the National Council of Scientific Research in Higher Education (Romanian Ministry of Education, Science and Youth), respectively the Sapientia Foundation (Cluj, Romania) to the authors.

6. REFERENCES

1. Kim, K., and Parlos, A.G., (2002), "Model-Based Fault Diagnosis of Induction Motors Using Non-Stationary Signal Segmentation," Mechanical Systems and Signal Processing, vol. 16, no. 2-3, pp. 223-253.
2. Nandi, S. and Toliyat, H.A., (1999), "Condition Monitoring and Fault Diagnosis of Electrical Machines – A Review," *Proceedings of the IEEE-IEMDC'99 Conference*, Seattle, pp. 219-221.
3. Thomson, W.T., and Gilmore, R.J., (2003), "Motor Current Signature Analysis to Detect Faults in Induction Motor Drives – Fundamentals, Data Interpretation, and Industrial Case Histories," *Proceedings of 32nd Turbomachinery Symposium*, Texas, A&M University, USA.
4. Milimonfared, J. et al., (1999), "A Novel Approach for Broken Rotor Bar Detection in Cage Induction Motors," *IEEE Transactions on Industry Applications*, vol. 35, no. 5, pp. 1000-1006.
5. Szabó, L., Bíró, K.Á., and Dobai, J.B., (2003), "Non-Invasive Rotor Bar Faults Diagnosis of Induction Machines Using Virtual Instrumentation," *Oradea University Annals*, Electrotechnical Section, pp. 313-320.
6. Marsh, D., (2003), "Virtual Instruments Drive Test Standards," *EDN Europe*, vol. 10, no. 2, 2003.
7. Szabó, L., Bíró, K.Á., and Dobai, J.B., (2003), "On the Rotor Bar Faults Detection in Induction Machines," *Proceedings of the International Scientific Conference MicroCAD '2003*, Miskolc (Hungary), Section J (Electrotehnics and Electronics), pp. 81-86.